# Estimation of Cardiac Fibre Direction Based on Activation Maps

de Vries, Johannes W.; Sun, Miao; de Groot, Natasja M.S.; Hendriks, Richard C.

**DOI**
10.1109/ICASSP49357.2023.10095692

**Publication date**
2023

**Document Version**
Final published version

**Published in**
Proceedings of the ICASSP 2023 - 2023 IEEE International Conference on Acoustics, Speech and Signal Processing (ICASSP)

ICASSP 2023 - 2023 IEEE International Conference on Acoustics, Speech and Signal Processing (ICASSP) | 978-1-7281-6327-7/23/$31.00 ©2023 IEEE | DOI: 10.1109/ICASSP49357.2023.10095692

# ESTIMATION OF CARDIAC FIBRE DIRECTION BASED ON ACTIVATION MAPS

*Johannes W. de Vries*, Miao Sun*, Natasja M.S. de Groot† and Richard C. Hendriks**

* Signal Processing Systems group, Delft University of Technology, the Netherlands
† Department of Cardiology, Erasmus University Medical Center, the Netherlands

## ABSTRACT

Estimating tissue conductivity parameters from electrograms (EGMs) could be an important tool for diagnosing and treating heart rhythm disorders such as atrial fibrillation (AF). One of these parameters is the fibre direction, often assumed to be known in conductivity estimation methods. In this paper, a novel method to estimate the fibre direction from EGMs is presented. This method is based on local conduction slowness vectors of a propagating activation wave. These conduction slowness vectors follow an elliptical pattern that depends on the underlying conductivity parameters. The fibre direction and conductivity anisotropy ratio can therefore be estimated by fitting an ellipse to the conduction slowness vectors. Applying the presented method on simulated data shows that it can estimate the fibre direction more accurately than existing methods, and that its performance depends mostly on the range of wavefront directions present in the measurement area. The main advantage of the presented method is that it still functions relatively well in the presence of conduction blocks, as long as the surrounding tissue is approximately homogeneous.

***Index Terms***— Anisotropy, atrial fibrillation, conduction velocity, fibre direction, local activation time

## 1. INTRODUCTION

Contractions of the heart are induced by action potentials propagating through the cardiac tissue. These action potentials consist of a rapid depolarisation of the transmembrane potential of a muscle cell (myocyte), causing the cell to contract and neighbouring cells to depolarise as well. The electrical propagation through the cardiac cells that follows is determined by the tissue conductivity. Due to the complex composition of cardiac tissue, the conductivity is generally inhomogeneous and orthotropic, with the main direction of propagation aligned with the fibre direction.

Impaired electrical conductivity in pathological tissue plays an important role in cardiac electrophysiology as it gives rise to heart rhythm disorders such as atrial fibrillation (AF) [1]. The impaired conductivity hinders a smooth contraction of the atria, which has several long-term health risks such as an increased risk of heart failure and stroke. Being able to estimate the local atrial tissue conductivity from electrogram (EGM) recordings could be an important tool in diagnosing and treating AF.

The inverse problem of estimating local tissue conductivity parameters from EGM measurements, however, is an ill-posed and highly challenging task due to high dimensionality, nonlinearity and stochasticity. Furthermore, most estimation approaches focus on finding a single set of homogeneous parameters for the whole tissue, which does not facilitate localisation of areas with impaired conductivity. Recently, some methods have been developed that estimate conductivity parameters locally [2]–[4]. Although these methods perform relatively well, they depend on a number of parameters that are assumed to be known. One of these parameters is the fibre direction, which influences the effective conductivity due to the orthotropic nature of the tissue. A method to estimate this fibre direction was developed by Roney *et al.* [5] in 2019, based on fitting elliptical wavefronts to local activation times (LATs). This method does not perform well, however, in the presence of conduction blocks due to wavefronts breaking up. Another method was used by Houben *et al.* in 2004 [6], based on conduction velocity properties. This paper presents a novel method to estimate the fibre direction from LATs based on reciprocal conduction velocity, aiming to improve the estimation accuracy while still performing well for tissue with conduction blocks.

## 2. PHYSIOLOGICAL MODELS

Cardiac tissue is a composite tissue and consists mainly of muscle cells, capable of providing tension. The contraction of these cells is triggered by electrical depolarisation. Specialised cells in the sinoatrial node can generate an electrical impulse: the action potential. This action potential consists of a rapid depolarisation, activating the cell contraction, and a slower repolarisation. Due to intercellular coupling, the depolarisation also induces depolarisation in neighbouring muscle cells. Because of the delay in this coupling, each myocyte activates at a different time, known as the LAT. A propagating depolatisation wave follows through the tissue. The orthotropic nature of the tissue conductivity means that the conduction velocity of the wave is also orthotropic and the wavefronts are therefore usually elliptical in shape.

### 2.1. Monodomain model

To obtain a mathematical model of the electrophysiology of the heart, cardiac tissue can be approximated as one continuous and homogeneous domain. This domain is characterised by a location dependent conductivity tensor $\mathbf{\Sigma}$ and transmembrane potential $V$. Combining Ohm's law, conservation of current and a physiological decomposition of the transmembrane current [7] leads to the partial differential equation known as the monodomain model. A detailed derivation of this equation can be found in [8]. The continuous model can be discretised for computational purposes. The tissue is approximated by a two dimensional regular lattice of $N_x \times N_y = N$ nodes, indexed by $n_x \in \{1, \ldots, N_x\}$ and $n_y \in \{1, \ldots, N_y\}$, that can either represent cells or groups of cells. Assuming a regular lattice allows for the finite difference method (FDM) to be used in place of continuous partial derivatives. It has been shown that the monodomain model describes the caridac electrophysiology accurately, as long as no injection of extracellular current is involved [9]–[11].

### 2.2. Conductivity tensor

The propagation of the depolarisation wave strongly depends on the electrical conductivity of the tissue. Tissue conductivity is an orthotropic property [12], and can therefore be described as a symmetric tensor. When considering two dimensional tissue, this tensor is a $2 \times 2$ symmetric matrix. An intuitive interpretation follows from applying an eigendecomposition, given by

$$\mathbf{\Sigma} = \begin{pmatrix} \cos\zeta & -\sin\zeta \\ \sin\zeta & \cos\zeta \end{pmatrix} \begin{pmatrix} \sigma_\ell & 0 \\ 0 & \alpha_\sigma \sigma_\ell \end{pmatrix} \begin{pmatrix} \cos\zeta & \sin\zeta \\ -\sin\zeta & \cos\zeta \end{pmatrix}. \tag{1}$$

Here, $\sigma_\ell$ is the conductivity in longitudinal direction, $\alpha_\sigma$ is the anisotropy ratio such that $\alpha_\sigma \sigma_\ell$ represents the conductivity in transverse direction, and $\zeta$ is the angle of longitudinal conductivity relative to the $x$-axis of the measurement frame of reference. Due to the spatial organisation of the cells, longitudinal conductivity is along the local fibre direction of the tissue. This means that $\zeta$ corresponds to the local fibre direction.

### 2.3. Local activation time & conduction slowness

When a depolarisation wave passes through the tissue, each cell is activated at a different time. The LAT $\tau$ of a cell is found from the transmembrane potential either as the instant the $-40\,\mathrm{mV}$ threshold is passed or as the instant the time derivative is maximal. In practice, however, transmembrane potentials are only known indirectly through the measured EGM potentials, and the LATs have to be estimated [13]. The complete set of estimated LATs provides a discrete, approximate activation map of the tissue area.

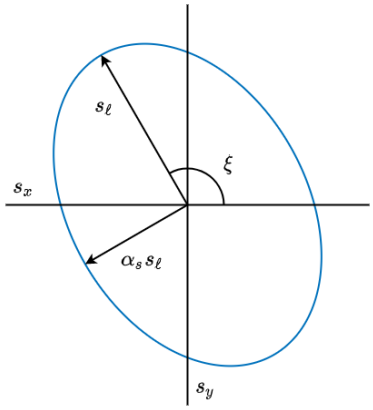


**Fig. 1**: Ellipse representation of conduction slowness with $\alpha_s = \frac{1}{\sqrt{2}}$ and $\xi = \frac{2}{3}\pi\,\mathrm{rad}$.

The wavefront velocity is known as the conduction velocity, and its reciprocal quantity is defined here as the conduction slowness. Conduction slowness is an interesting wave property with a strong dependence on the conductivity parameters. Similarly to tissue conductivity, conduction slowness is orthotropic [14] and can be represented as an ellipse in the conduction slowness space. The orientation of this ellipse is the longitudinal conduction slowness direction $\xi$, which aligns with the transversal conductivity direction such that

$$\xi = \zeta + \frac{1}{2}\pi. \tag{2}$$

The semiminor to semimajor axis ratio is the conduction slowness anisotropy ratio $\alpha_s$, which is related to the conductivity anisotropy ratio as [15]

$$\alpha_s^2 = \alpha_\sigma. \tag{3}$$

The radius of the ellipse in the wavefront direction equals the effective conduction slowness of that wavefront. Figure 1 shows an example of this ellipse representation.

## 3. PROPOSED METHOD

The local conduction slowness of a node in an activation map is a vector obtained from the gradient of the activation map:

$$\boldsymbol{s}(x,y) = \begin{pmatrix} s_x(x,y) \\ s_y(x,y) \end{pmatrix} = \boldsymbol{\nabla}\tau(x,y). \tag{4}$$

Because activation maps are discrete, this gradient can be numerically approximated using the FDM. The local conduction slownesses can be represented as points in the conduction slowness space, and for a homogeneous area of tissue, these points roughly align with the aforementioned ellipse. The fibre direction and conductivity anisotropy ratio can therefore be estimated from an activation map by fitting a modelled ellipse to the conduction slowness points.

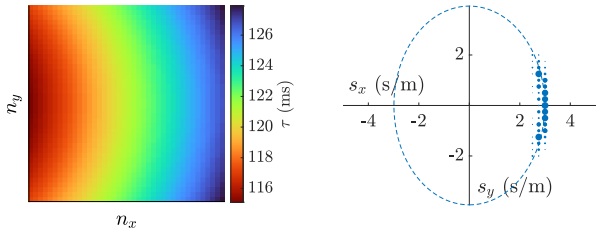


(a) (b)

**Fig. 2**: Simulated (a) activation map and (b) corresponding local conduction slowness points and fitted ellipse (dashed line).

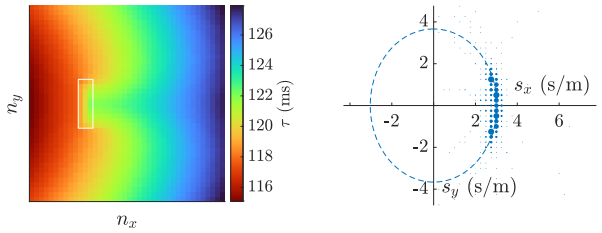


(a) (b)

**Fig. 3**: Simulated (a) activation map and (b) corresponding local conduction slowness points and fitted ellipse (dashed line), for tissue with conduction block (white outline). Some outliers, with magnitudes up to $15\,\mathrm{s/m}$, are not visible here.

The general form equation for the ellipse is given by

$$p_1 s_x^2 + p_2 s_x s_y + p_3 s_y^2 = 1. \tag{5}$$

Using the ellipse fitting approach in [16], the local conduction velocity coordinates of all $N$ nodes are stored in design matrix

$$\boldsymbol{D} = \begin{pmatrix} s_{x,1}^2 & s_{x,1}s_{y,1} & s_{y,1}^2 \\ \vdots & \vdots & \vdots \\ s_{x,N}^2 & s_{x,N}s_{y,N} & s_{y,N}^2 \end{pmatrix} \tag{6}$$

such that the fitting problem can be expressed as

$$\min_{\boldsymbol{p}} \quad \|\boldsymbol{D}\boldsymbol{p} - \boldsymbol{1}\|^2. \tag{7}$$

This problem has the closed form least squares solution

$$\boldsymbol{p} = \boldsymbol{D}^{\dagger}\boldsymbol{1}. \tag{8}$$

where $\dagger$ represents the Moore–Penrose inverse. Converting these coefficients to the estimated conduction slowness parameters, and applying (2) and (3), results in

$$\hat{\zeta} = \arctan\left(\frac{p_3 - p_1 - \sqrt{(p_3-p_1)^2 + p_2^2}}{p_2}\right) + \frac{1}{2}\pi \tag{9}$$

and

$$\hat{\alpha}_\sigma = \frac{p_1 + p_3 - \sqrt{(p_3-p_1)^2 + p_2^2}}{p_1 + p_3 + \sqrt{(p_3-p_1)^2 + p_2^2}}. \tag{10}$$

A simulation example is shown in Figure 2, which shows an activation map and the corresponding local conduction slowness space, for homogeneous tissue with $\zeta = 0\,\mathrm{rad}$ and $\alpha_\sigma = \frac{1}{2}$. The local conduction slowness vectors are plotted as points, with relative area sizes corresponding to the amount of overlapping vectors. The vectors closely follows an elliptical shape, and the range of vector directions equals the range of wavefront directions present in the considered tissue area. The fitted ellipse, found from (5) using (8), is plotted as well. The resulting estimates are $\hat{\zeta} = 0\,\mathrm{rad}$ and $\hat{\alpha}_\sigma = 0.57$.

When conduction blocks are present in the tissue, the elliptical wavefronts break up and wakes form behind the conduction block areas. This effect can be observed in the activation map of the simulation example in Figure 3. In this example, the same tissue is simulated except for the presence of a conduction block area. Although most local conduction slowness vectors still roughly follow the underlying ellipse, a notable number of outliers is present as well. A first cause is the lower conductivity at the conduction block areas, which causes high magnitudes of the local conduction slowness. A second cause of the outliers is a thin trail of low magnitudes at the centre of the wakes behind conduction block area. This is where two wavefronts collide, characterised by a near-zero conduction slowness. Although these two groups of local conduction slowness vectors disrupt the estimation, most of the area in the wakes still behaves identical to the rest of the tissue but with altered wavefront directions. As long as conduction blocks are not too large or prevalent, outlier detection methods can be used to remove these unusable vectors. In this paper, outliers are classified as vectors with a magnitude more than three scaled median absolute deviations away from the median. The resulting estimates for the tissue with conduction blocks are $\hat{\zeta} = 0.00093\pi\,\mathrm{rad}$ and $\hat{\alpha}_\sigma = 0.69$.

## 4. SIMULATION RESULTS

To test the proposed estimation method, activation maps were simulated[1] using the monodomain model and the Courtemanche model [17]. LATs are found from the transmembrane potentials as the time instant the potentials reach $-40\,\mathrm{mV}$. The area that is externally stimulated is $10 \times 10$ cells, chosen to exceed the liminal area [18]. The distance between measurement and stimulus area $d$, measurement area size $A$ and true fibre direction $\zeta$ are all varied between simulations. Simulated tissues both without and with conduction blocks are used, similar to the setup for the activation maps in Figures 2 and 3 respectively. The fibre direction estimation errors are expressed as absolute errors: $\mathcal{E}_\zeta = |\hat{\zeta} - \zeta|$.

The largest factor influencing the estimation accuracy is the range of wavefront directions present in the measurement area. A larger range leads to a more accurate ellipse fitting

[1] MATLAB codes of the simulation and proposed estimation method are available at the repository of `sps.ewi.tudelft.nl`.

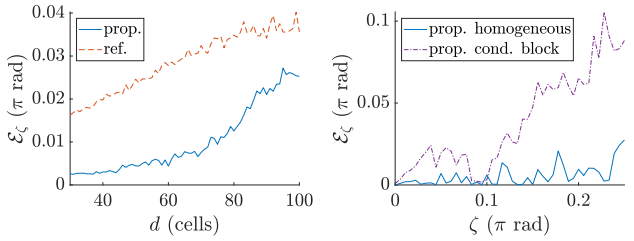


(a) (b)

**Fig. 4**: Fibre direction estimation error as a function of (a) the stimulus–measurement area distance (for the proposed and reference method [6]), and (b) the true fibre direction (for tissue without and with a conduction block area).

and in turn to a higher estimation accuracy. The range of available wavefront directions is mainly determined by the stimulus–measurement area distance and the measurement area size. Figure 4a (solid blue line) shows estimation errors as a function of the stimulus–measurement area distance, for homogeneous tissue with $A = 40 \times 40$ cells and $\alpha_\sigma = 0.5$, and averaged over a range of fibre directions. As can be observed, the estimation performance generally increases when measurements are taken closer to the stimulus. A similar effect is obtained when the measurement area is increased.

The propagation direction relative to the true fibre direction also influences the wavefront direction range, and in turn the estimation accuracy. This is shown in Figure 4b (solid blue line), where a similar simulation as for Figure 4a was performed, but as a function of the true fibre direction and with a constant stimulus–measurement area distance of $d = 40$. As the true fibre direction diverges from $0\,\mathrm{rad}$ (the general propagation direction), the estimation error increases on average. In practice, only small deviations between fibre direction and wave origin direction would be expected, which favours smaller estimation errors for this method.

When a conduction block area is present in the tissue, the estimation results generally decrease slightly. An example is shown by the dashed orange line in Figure 4b. The amount of performance decrease depends on the size and amount of conduction block areas. In case of approximately planar wavefronts, however, the presence of conduction blocks can actually increase the performance. This is because the wavefront direction range can increase due to the wavefront breakup around the block.

In practice, EGMs indirectly record transmembrane potentials of groups of cells instead of individual cells. The decreased spatial resolution of resulting activation maps decreases the resolution of the conduction slowness vectors. This does not influence the estimation accuracy much as the range of wavefront directions is largely unaffected, and the conduction slowness vectors roughly follow the same ellipse. This also holds true for decreased temporal resolution and mild LAT estimation errors, which similarly decrease the conduction slowness resolution. When conduction blocks are present and the spatial resolution is too low, however, the activation times around conduction blocks become blurred. This decreases the proportion of useful activation times and might hinder outlier detection as well.

The proposed method mostly performs better than the method used by Houben *et al*. In general, the method by Houben *et al.* has absolute estimation errors around $0.015\pi\,\mathrm{rad}$ higher than the proposed method. An example comparison is shown in Figure 4a.

## 5. CONCLUSION

The fibre direction is a tissue parameter that determines the direction of longitudinal conduction of the tissue and appears in the spatial differential term of the monodomain equation. A novel method was presented that estimates the fibre direction of atrial tissue based on local conduction slownesses found from LATs. Due to the relation between the conduction slowness and conductivity, the fibre direction and conductivity anisotropy ratio of an area of tissue can be estimated from these local conduction slownesses. Simulations were performed to test the estimation method under different circumstances. These simulations show the estimation method works well, even in the presence of a conduction block area. The main factor influencing the estimation performance is the range of wavefront directions present in the measurement area. Mild reductions in spatial and temporal resolution of activation maps also barely affect the estimation accuracy.

The fibre direction estimation method by Roney *et al.* [5] is based on applying elliptical wavefront fitting to an activation map directly. Because wavefronts are not elliptical of shape in the presence conduction blocks, this method does not work in the context of AF and the conductivity estimation methods of [2]–[4]. Another fibre direction estimation method has been used by Houben *et al.* [6]. The main difference between this method and the proposed method is whether conduction velocities or conduction slownesses are used for estimation. A comparison of simulation results shows that the method based on conduction slowness provides more accurate estimates. The reason seems to be that the conduction slowness directly follows from the gradient of the LATs, as seen in (4). By additionally taking reciprocal magnitudes, the elliptical nature is lost. Furthermore, the method by Houben *et al.* does not make use of the anisotropy ratio relation of (3), instead assuming both ratios to be equal. This decreases the anisotropy ratio estimation accuracy.

The main goal of the presented estimation method is to provide accurate fibre direction estimates, even in cases of tissue with conduction blocks. The performed simulations show that this goal has been achieved and that estimation accuracies have increased relative to existing methods. The presented method is therefore a considerable improvement upon existing fibre direction estimation algorithms based on EGMs.

## 6. REFERENCES


[1] T. M. Munger, L. Q. Wu, and W. K. Shen, "Atrial fibrillation," *J. Biomed. Res.*, vol. 28, no. 1, pp. 1–17, Jan. 2014.

[2] B. Abdi, R. C. Hendriks, A. van der Veen, and N. M. S. de Groot, "A compact matrix model for atrial electrograms for tissue conductivity estimation," *Comput. Biol. Med.*, vol. 107, pp. 284–291, May 2019.

[3] M. Sun, N. M. S. de Groot, and R. C. Hendriks, "Cardiac tissue conductivity estimation using confirmatory factor analysis," *Comput. Biol. Med.*, vol. 135, Aug. 2021, Art. no. 104604.

[4] M. Sun, N. M. S. de Groot, and R. C. Hendriks, "Joint cardiac tissue conductivity and activation time estimation using confirmatory factor analysis," *Comput. Biol. Med.*, vol. 144, May 2022, Art. no. 105393.

[5] C. H. Roney et al., "A technique for measuring anisotropy in atrial conduction to estimate conduction velocity and atrial fibre direction," *Comput. Biol. Med.*, vol. 104, pp. 278–290, Jan. 2019.

[6] R. P. M. Houben, N. M. S. de Groot, J. L. R. M. Smeets, A. E. Becker, F. W. Lindemans, and M. A. Allessie, "S-wave predominance of epicardial electrograms during atrial fibrillation in humans: Indirect evidence for a role of the thin subepicardial layer," *Heart Rhythm*, vol. 1, no. 6, pp. 639–647, Dec. 2004.

[7] A. L. Hodgkin and A. F. Huxley, "A quantitative description of membrane current and its application to conduction and excitation in nerve," *J. Phys.*, vol. 117, no. 4, pp. 500–544, Aug. 1952.

[8] R. H. Clayton et al., "Models of cardiac tissue electrophysiology: Progress, challenges and open questions," *Prog. Biophys. Mol. Biol.*, vol. 104, no. 1–3, pp. 22–48, Jan. 2011.

[9] M. Potse, B. Dubé, J. Richer, A. Vinet, and R. M. Gulrajani, "A comparison of monodomain and bidomain reaction–diffusion models for action potential propagation in the human heart," *IEEE Trans. Biomed. Eng.*, vol. 53, no. 12, pp. 2425–2435, Dec. 2006.

[10] B. F. Nielsen, T. S. Ruud, G. T. Lines, and A. Tveito, "Optimal monodomain approximations of the bidomain equations," *Appl. Math. Comput.*, vol. 184, no. 2, pp. 276–290, Jan. 2007.

[11] Y. Coudière, Y. Bourgault, and M. Rioux, "Optimal monodomain approximations of the bidomain equations used in cardiac electrophysiology," *Math. Models Methods Appl. Sci.*, vol. 24, no. 6, pp. 1115–1140, Jun. 2014.

[12] D. A. Hooks, M. L. Trew, B. J. Caldwell, G. B. Sands, I.J. LeGrice, and B. H. Smaill, "Laminar arrangement of ventricular myocytes influences electrical behavior of the heart," *Circ. Res.*, vol. 101, no. 10, pp. e103–e112, Nov. 2007.

[13] C. D. Cantwell, C. H. Roney, F. S. Ng, J. H. Siggers, S. J. Sherwin, and N. S. Peters, "Techniques for automated local activation time annotation and conduction velocity estimation in cardiac mapping," *Comp. Biol. Med.*, vol. 65, pp. 229–242, Oct. 2015.

[14] T. Sano, N. Takayama, and T. Shimamoto, "Directional difference of conduction velocity in the cardiac ventricular syncytium studied by microelectrodes," *Circ. Res.*, vol. 7, no. 2, pp. 262–267, Mar. 1959.

[15] L. Clerc, "Directional differences of impulse spread in trabecular muscle from mammalian heart," *J. Phys.*, vol. 255, no. 2, pp. 335–346, Feb. 1976.

[16] D. Hart and A. J. Rudman, "Least-squares fit of an ellipse to anisotropic polar data: Application to azimuthal resistivity surveys in karst regions," *Comput. Geosci.*, vol. 23, no. 2, pp. 189–194, Mar. 1997.

[17] M. Courtemanche, R. J. Ramirez, and S. Nattel, "Ionic mechanisms underlying human atrial action potential properties: insights from a mathematical model," *Amer. J. Physiol. Heart Circ. Physiol.*, vol. 275, no. 1, pp. H301–H321, Jul. 1998.

[18] B. M. Ramza, R. C. Tan, T. Osaka, and R. W. Joyner, "Cellular mechanism of the functional refractory period in ventricular muscle," *Circ. Res.*, vol. 66, no. 1, pp. 147—-162, Jan. 1990.